The Abnormal Indian Summer Monsoon of 2000

R. KRISHNAN, M. MUJUMDAR, V. VAIDYA, K. V. RAMESH, AND V. SATYAN

Indian Institute of Tropical Meteorology, Pune, India

(Manuscript received 12 December 2001, in final form 23 September 2002)

ABSTRACT

Diagnostic analysis of observations and a series of ensemble simulations using an atmospheric general circulation model (GCM) have been carried out with a view to understanding the processes responsible for the widespread suppression of the seasonal summer monsoon rainfall over the Indian subcontinent in 2000. During this period, the equatorial and southern tropical Indian Ocean (EQSIO) was characterized by persistent warmer than normal sea surface temperature (SST), increased atmospheric moisture convergence, and enhanced precipitation. These abnormal conditions not only offered an ideal prototype of the regional convective anomalies over the subcontinent and Indian Ocean, but also provided a basis for investigating the causes for the intensification and maintenance of the seasonal anomaly patterns.

The findings of this study reveal that the strengthening of the convective activity over the region of the southern equatorial trough played a key role in inducing anomalous subsidence over the subcontinent and thereby weakened the monsoon Hadley cell. The leading empirical orthogonal function (EOF) of the intraseasonal variability of observed rainfall was characterized by a north–south asymmetric pattern of negative anomaly over India and positive anomaly over the region of the EQSIO and accounted for about 21% of the total rainfall variance during 2000. The GCM-simulated response to forcing by SST anomalies during 2000 is found to be consistent with observations in reasonably capturing the seasonal monsoon anomalies and the intraseasonal variability. Further, it is shown from the GCM experiments that the warm Indian Ocean (IO) SST anomalies influenced the regional intraseasonal variability in a significant manner by favoring higher probability of occurrence of enhanced rainfall activity over the EQSIO region and, in turn, led to higher probability of occurrence of dry spells and prolonged break-monsoon conditions over the subcontinent. In particular, the simulated break-monsoon anomaly pattern of decreased rainfall over the subcontinent and increased rainfall over the EQSIO is shown to intensify and persist in response to the IO SST anomalies during 2000. These results clearly bring out the significance of the IO SST anomalies in altering the regional intraseasonal variability and thereby affecting the seasonal mean monsoon. Further studies will be required in order to investigate the detailed physical mechanisms that couple the variability of convection over the IO region with the local SST boundary forcing and the large-scale monsoon dynamics.

1. Introduction

The south Asian summer monsoon circulation, occurring every year from June to September, is one of the most spectacular seasonal phenomena on the globe. Despite the remarkable consistency in the seasonal reversal of the wind patterns, it is well known that the summer monsoon rainfall over the Indian subcontinent exhibits considerable interannual variability (Parthasarathy et al. 1995). Particularly noteworthy is the recent case of abnormally low Indian monsoon rainfall in 2000. Severe drought conditions prevailed over a large area covering the plains of central and north India where the monsoon rainfall was deficient by more than 25% of the normal (Fig. 1a). The total rainfall for the monsoon season of 2000 over the whole of the country was about 8% below the long-term climatological normal.[1] There are several compelling reasons for undertaking the 2000 monsoon case study. First, the precipitation decrease was widespread. Extreme drought conditions were not confined merely to the plains of north-central India but also extended over areas of Pakistan and southwest Asia (Barlow et al. 2002) so that the large rainfall reduction by the end of September 2000 produced an adverse impact on the water availability over the south Asian region. The second important aspect was the occurrence of prolonged break (inactive) spells during the 2000 monsoon rainy season. The daily time series of the all-India summer monsoon precipitation (Fig. 1b) shows three major break spells (i.e., the first one in the third week of June; the second was an intense and long dry spell extending from the third week of July until the

Corresponding author address: R. Krishnan, Indian Institute of Tropical Meteorology, Dr. Homi Bhabha Road, Pashan, NCL-Post, Pune 411 008, India.
E-mail: krish0365@yahoo.com

[1] The India Meteorological Department defines a monsoon drought when the all-India summer monsoon rainfall during a given year is deficient by more than 10% of the climatological normal.

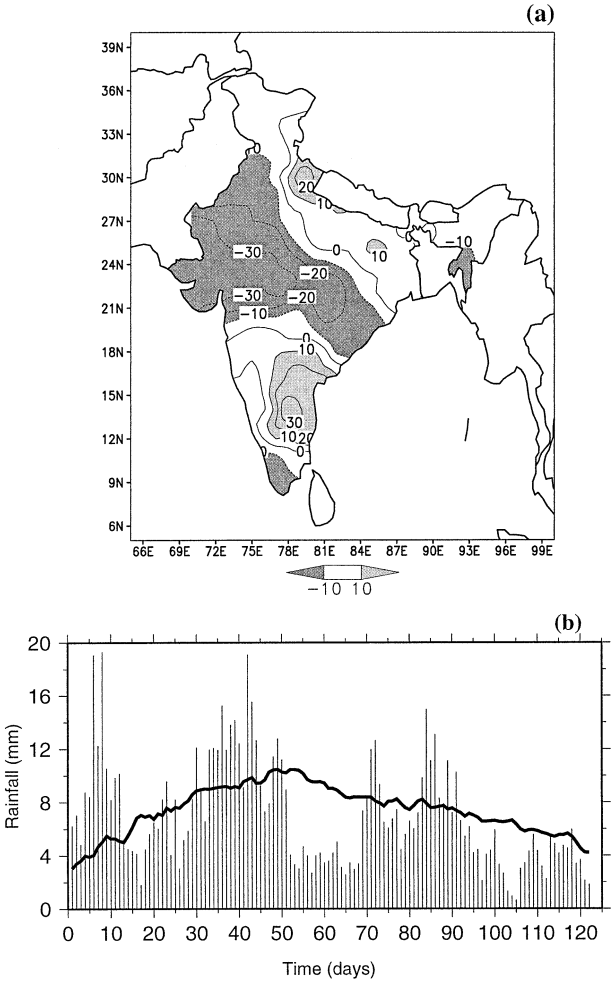

FIG. 1. (a) The anomalies of the Jun–Sep (JJAS) rainfall (% departure from normal) over India during 2000 based on rain gauge observations over Indian stations (http://www.tropmet.res.in). The anomalies are obtained by subtracting the long-term climatological normals over different stations. The magnitude of negative departures associated with severe drought conditions over northwest and central India (Rajasthan, Saurashtra and Kutch, Gujarat and Madhya Pradesh) exceed more than 25%. Only very small pockets such as east peninsular India and the hills of West Uttar Pradesh received above normal rainfall. (b) Bar graph showing the daily all-India rainfall (mm) for the period 1 Jun–30 Sep 2000. The solid line is the daily climatological normal.

second week of August; and the next break spell occurred in the second and third weeks of September). These three break spells during 2000 have also been verified from the Climate Prediction Center (CPC) Merged Analysis of Precipitation (CMAP) pentadal rainfall dataset by Krishnan et al. (2001). In addition, they examined daily charts of surface pressure departures over Indian stations and confirmed that the prolonged break monsoon condition during 2000 was associated with above normal pressure departures of the order of 4 hPa over the plains of north-central India. It is known that enhanced probability of occurrence of break conditions in a certain year could result in weaker than normal seasonal mean monsoon rainfall (Goswami and Ajaya Mohan 2001). Therefore, it is pertinent to examine the agents that were responsible for inducing the long-lasting behavior of the monsoon break spells in 2000.

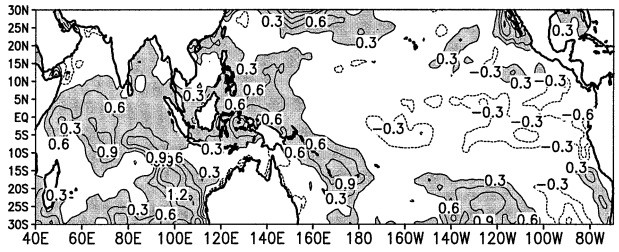

FIG. 2. The observed SST (°C) anomaly for JJAS 2000 from the monthly OISST dataset. Anomalies are with respect to the OISST climatology (Smith and Reynolds 1998) for the base period (1961–90).

The third point about the 2000 summer monsoon is the nature of tropical SSTs that prevailed during that season. It is known that a majority of monsoon droughts in the past have occurred in conjunction with El Niño events in the Pacific Ocean (Sikka 1999). Previous studies have pointed out that enhanced convection associated with warm SST anomalies in the tropical central-eastern Pacific Ocean can induce anomalous subsidence of the east–west Walker circulation over the Indian region and thereby suppress the monsoon rainfall (Palmer et al. 1992). Numerous studies have documented the relationship between El Niño–Southern Oscillation (ENSO) and the Indian monsoon rainfall (Pant and Parthasarathy 1981; Rasmusson and Carpenter 1983; Shukla and Paolino 1983). In contrast to most of the earlier droughts, the widespread decrease of monsoon rainfall in 2000 was, however, not related to El Niño conditions in the Pacific Ocean. The absence of an El Niño event during 2000 is clearly evident from the plot of observed SST anomalies (Fig. 2) that shows weak negative anomalies in the equatorial central-eastern Pacific Ocean. On the other hand, the tropical Indian Ocean (IO) was characterized by warm SST anomalies extending longitudinally across much of the ocean basin. The maximum value of the SST anomaly around 55°–65°E to the south of the equator was close to 1°C. Warm SST anomalies can also be noticed to the south of 10°S in the central-eastern IO in Fig. 2. By examining the monthly fields, we have confirmed that the positive SST anomalies in the tropical IO persisted during the entire monsoon season.

Convection variability over the tropical IO and the monsoon region remain ambiguous in many aspects. For instance, while it is known that convection tends to increase over the equatorial IO during monsoon breaks (Krishnan et al. 2000; Goswami and Ajaya Mohan 2001), it is not clear how the distribution of convection patterns during monsoon breaks is affected by SST anomalies in the IO. One of the main reasons for the

complexity of this problem is the inherent nonlinear relationships among SST, convection, and atmospheric dynamics (Zhang 1993). Nevertheless, the situation that prevailed during 2000 provided an excellent opportunity to examine some of the regional issues in greater depth. Especially, the occurrence of prolonged monsoon breaks over India, in combination with the warm SST anomalies in the tropical Indian Ocean and the lack of El Niño conditions in the Pacific Ocean, offered a naturally conductive setting to concentrate on the impact of the IO SST anomalies on the regional-scale convection. In the past, there have been a few studies dealing with the influence of IO SST anomalies on the summer monsoon. Shukla (1975) examined the impact of cold SST anomalies, in the western Arabian Sea and the Somali coast, on monsoon circulation and rainfall. His results showed a decrease of rainfall over India, which he attributed to a decrease of local evaporation and reduction in the cross-equatorial moisture flux. Washington et al. (1977) studied the summer monsoon response to different types of idealized SST anomalies in the tropical IO. Their results indicated an increase in rainfall and vertical velocity over the warm SST anomaly. However, the simulated monsoon rainfall and wind anomalies obtained in their experiments were not statistically significant. In a more recent study, Chandrasekar and Kitoh (1998) carried out experiments using the Meteorological Research Institute (MRI) GCM in order to examine the sensitivity of the monsoon circulation and rainfall to anomalous SST in the tropical IO. They noted that rainfall increased (decreased) over the IO region of warm (cold) SST anomaly. In contrast, the seasonal rainfall over the Indian land region showed a decrease (increase); accompanied by a weakening (strengthening) of the cross-equatorial flow in their warm (cold) SST anomaly experiment. One of the shortcomings of their study was the lack of observational justification for the idealized IO SST anomaly, which was held fixed in their model integrations. Since a GCM response can be quite sensitive to the distribution of SST, it is essential that the specified SST boundary forcing is as realistic as possible so that the model simulation can be evaluated objectively (Palmer et al. 1992). Second, Chandrasekar and Kitoh (1998) only speculated about the possible impact of SST anomalies on the convection over the monsoon region; however, their model simulations did not explicitly provide an explanation for the modifications of the intraseasonal active/break monsoon spells due to the SST forcing. Given that the monsoon intraseasonal variability significantly accounts for the seasonal anomalies in a certain year (Goswami and Ajaya Mohan 2001), it is not obvious how the subseasonal timescale variability responds to SST anomalies in the tropical IO. A consistent description of the linkage between the tropical IO SST anomalies and the intraseasonal variability of convection is essential for interpreting the persistence of seasonal mean monsoon anomalies as in 2000.

The primary objective of this paper is to understand the factors that contributed to the maintenance of the anomalous features associated with the monsoon droughtlike situation over India in 2000. One of the key issues concerns the influence of the warm tropical IO SST anomalies both on the large-scale monsoon circulation as well as on the intraseasonal variability of convection. In particular, special attention has been paid towards assessing the sensitivity of monsoon breaks to the IO SST forcing. Keeping these goals in mind, we have adopted a two-fold strategy that combines both diagnostic analysis of observed datasets and also numerical experiments using an atmospheric GCM.

a. Datasets used

Datasets from multiple sources have been employed for the present analysis. They consist of the subdivisional and all-India rainfall prepared by the Indian Institute of Tropical Meteorology (IITM), and the gridded rainfall dataset over both land and oceanic areas known as CMAP. The CMAP dataset is a product of merging rain gauge observations and precipitation estimates from satellites (Xie and Arkin 1997). The SST data used in our study is based on the optimum interpolated SST (OISST), which utilizes in situ and satellite-derived SSTs plus SSTs simulated by sea ice cover (Reynolds and Smith 1994). In addition, atmospheric parameters such as (winds, moisture, vertical velocity, rainfall, etc.) from the National Center for Environmental Prediction–National Center for Atmospheric Research (NCEP–NCAR) reanalysis dataset (Kalnay et al. 1996) have been used in our analysis.

b. Model and experimental details

The summer monsoon response to the IO SST anomalies during 2000 has been examined by performing four sets of 10-member ensemble integrations using the Center for Ocean–Land–Atmosphere (COLA) GCM. The four sets of experiments differ from each other with regard to the specification of the SST boundary forcing (see Table 1). The rationale behind carrying out the four sets of experiments is described in section 3. Each of these four sets in turn comprises 10 realizations, for which the GCM was integrated starting from 10 different initial conditions. The observed global atmospheric conditions from NCEP reanalysis for 10 continuous days (22–31 May 2000) were processed in order to obtain the multiple initial conditions necessary for performing the ensemble runs. All the model experiments, starting from different initial conditions, go through 30 September 2000. Initial conditions for the land surface (soil moisture, snow cover, etc.) are set to climatological values. Linear time-interpolation of these parameters from the monthly climatologies provide the land surface initial conditions on a given date for starting the model integration. After commencement of the

TABLE 1. GCM experiments.

Experiment	SST boundary condition	Initial condition
CLIM		
Ten ensemble members CLIM (01, 02, 03, ... 10)	Observed climatological SST	Ten ICs corresponding to (22, 23, 24, ... 31) May 2000
GL2K		
Ten ensemble members GL2K (01, 02, 03, ... 10)	Observed climatological SST + anomalies of 2000 for global oceans	Ten ICs corresponding to (22, 23, 24, ... 31) May 2000
IO2K		
Ten ensemble members IO2K (01, 02, 03, ... 10)	Observed climatological SST + anomalies of 2000 for Indian Ocean only	Ten ICs corresponding to (22, 23, 24, ... 31) May 2000
NOIO		
Ten ensemble members NOIO (01, 02, 03, ... 10)	Observed climatological SST + anomalies of 2000 everywhere except Indian Ocean	Ten ICs corresponding to (22, 23, 24, ... 31) May 2000

integration, these land surface parameters are predicted by the model. The SST used for prescribing the boundary conditions in the GCM is based on the observed OISST (Reynolds and Smith 1994). The details of these initial and boundary conditions are presented in Table 1. The COLA GCM is a spectral model with horizontal resolution truncated at wavenumber 30 (triangular truncation T30) and consists of 18 unevenly spaced sigma levels in the vertical. The complete documentation of the model framework and the physical parameterization schemes used in the GCM are provided by Kinter et al. (1997). This GCM has been extensively used for monsoon studies (e.g., Fennessy et al. 1994; Krishnan et al. 1998; Kirtman and Shukla 2000; Mujumdar and Krishnan 2001).

2. Data analyses

a. Seasonal features

The south Asian monsoon circulation is classically portrayed as a gigantic sea breeze, that is, a meridional Hadley cell (Krishnamurti 1986) driven by atmospheric differential heating between the Asian land mass (to the north) and the oceans (to the south). This large-scale circulation is accompanied by the seasonal monsoon rains over the Indian subcontinent during June–September. The spatial distribution of the observed seasonal mean precipitation (Fig. 3a) shows two rainfall maxima—one over the Bay of Bengal and the other over the west coast of India. A secondary rainfall maximum is located over the equatorial IO. Also illustrated in Fig. 3a is the transport of water vapor from the oceanic areas into the Indian region by the cross-equatorial winds and southwest monsoon flow. The monsoon Hadley circulation is depicted by the meridional–vertical section of atmospheric circulation in Fig. 3b. The ascending branch of the Hadley cell is located to the north of 15°N and the descending branch can be seen over the southern Indian Ocean. This circulation is associated with southerlies in the lower levels and northerlies in the upper troposphere.

The anomalies of precipitation and moisture transport vector for the 2000 monsoon season are shown in Fig. 3c. Large negative rainfall anomalies can be seen over the west coast of India, the eastern Arabian Sea, and the Bay of Bengal. Also prominently seen is the rainfall decrease over north-central India by as much as 2–3 mm day^{-1}. The small pocket of increased rainfall over the northeast region is a typical feature known to be associated with weakening of the monsoon activity (Ramamurthy 1969; Dhar et al. 1984; Krishnamurthy and Shukla 2000). The widespread reduction of rainfall over the plains of India shown by the CMAP dataset (Fig. 3c) is broadly consistent with the precipitation anomalies in Fig. 1a, which are entirely based on observed in situ rainfall over Indian stations. The moisture transport vector (Fig. 3c) reveals anomalous easterlies over the Arabian Sea, the Indian subcontinent, the Bay of Bengal, Burma, Thailand, and Vietnam—indicative of the decrease of water vapor influx into the monsoon region. This restricted moisture transport and the anticyclonic anomaly over India and the Arabian Sea corroborate with the rainfall suppression over the region. A conspicuous feature in Fig. 3c is the elongated band of increased rainfall over the equatorial IO during the summer of 2000. This anomalous patch with a magnitude as large as 1.5 mm day^{-1} is located between 5°S–5°N and extends eastward from about 60°E as far as the Indonesian islands and the west Pacific. The (y–p) section (Fig. 3d) illustrates anomalous upward motions over the equatorial region and compensating subsidence over the northern side (10°–20°N). With regard to the anomalous vertical velocities over 10°–20°S in Fig. 3d, the following points are to be taken into consideration. Firstly, it is important to note that the climatological y–p circulation shows subsidence at these latitudes (Fig. 3b). However, this subsidence over the southern IO weakened during 2000 in association with the weakening of the large-scale monsoon Hadley cell and is consistent with the anomalous upward motions over the southern latitudes (Fig. 3d). The second point is that climatological rainfall at these latitudes is quite low

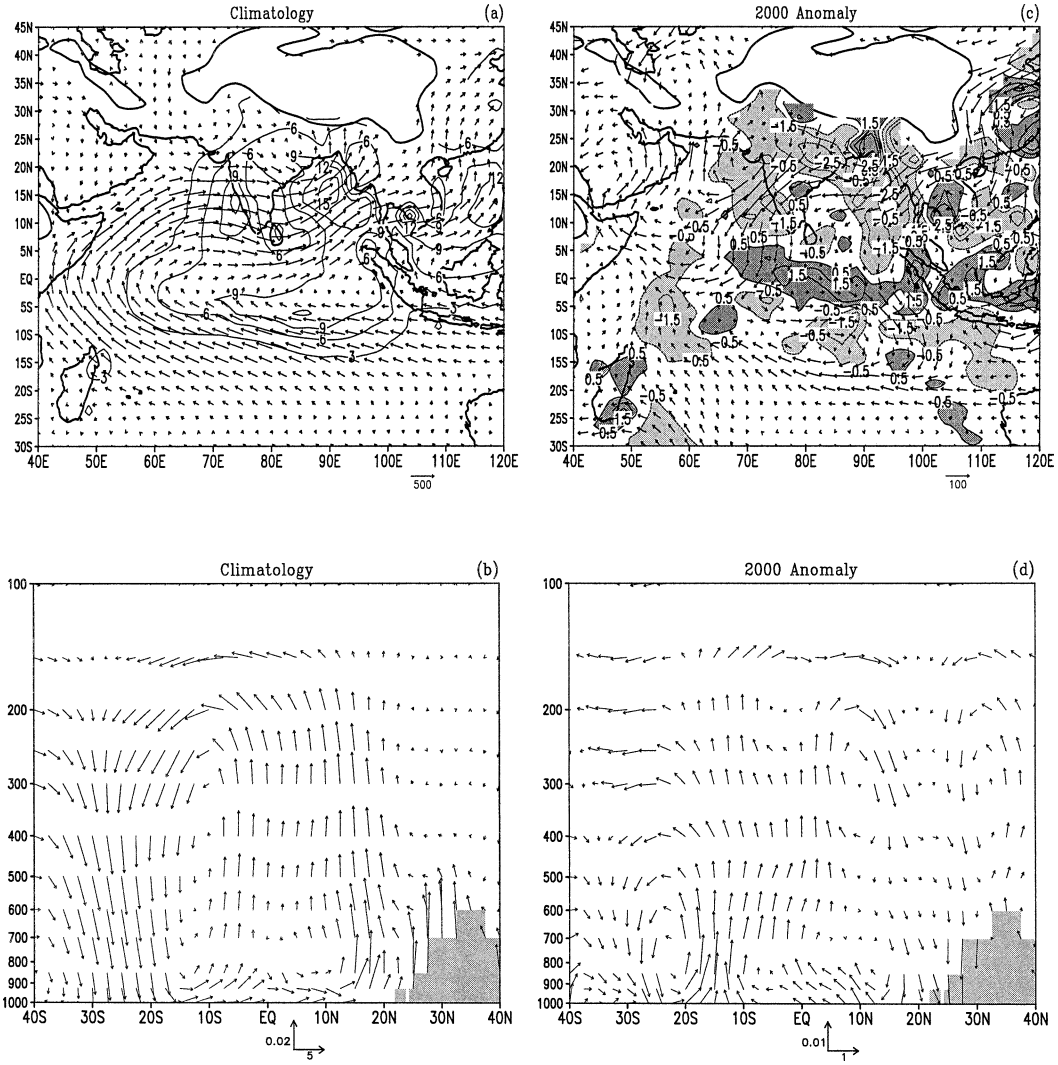

FIG. 3. (a) The JJAS climatological distribution of observed rainfall (with contour interval of 3 mm day^{-1}) and water vapor transport vector **Q** (kg m^{-1} s^{-1}); $\mathbf{Q} = 1/g \int_{P_u}^{P_s} q\mathbf{V}\, dP$ where g is the acceleration due to gravity and q is the specific humidity; P_u is 300 hPa and P_s is the surface pressure over a given geographical location. The rainfall is from the CMAP dataset; and **Q** is computed from NCEP reanalysis dataset. (b) The JJAS climatological monsoon Hadley cell shown by the cross section of meridional and vertical wind components averaged longitudinally between 50°–100°E. The vertical velocity (hPa s^{-1}) is taken with negative sign. (c) Same as in (a) except for 2000 anomalies. The contour interval for rainfall anomaly is 1 mm day^{-1}. (d) Same as in (b) except for 2000 anomalies.

(Fig. 3a) and the rainfall variability near 10°–20°S need not be entirely determined by the variations in the monsoon Hadley cell alone. Variations in local convection can affect the rainfall in this region. This may partly explain why the anomalous upward vertical velocities over 10°–20°S in Fig. 3d seem to be unrelated with the rainfall anomalies (Fig. 3c) at these latitudes. Moreover, note that the negative anomalies of the CMAP rainfall in the (10°–20°S) latitude belt, do not extend continously across the entire IO basin. Instead, they appear as negative patches (the first one near 55°E, the second near 85°E and the third around 105°E) having magnitudes in the range of 0.5–1.5 mm day^{-1}. However, the anomalous NCEP vertical velocity field in Fig. 3d, has been averaged longitudinally between 50°–100°E. Nevertheless, the main point from Fig. 3 is that the anomalous Hadley cell during 2000 provides dynamical support for the opposite polarity of convective anomalies over the subcontinent and the equatorial IO region.

b. Monsoon intraseasonal variability

It is well known that the southwest monsoon system exhibits vigorous intraseasonal fluctuations manifesting in the form of active/break rainfall spells (Krishnamurti and Bhalme 1976; Yasunari 1979; Sikka and Gadgil 1980; Krishnamurti and Subrahmanyam 1982; Krishnan et al. 2000; Goswami and Ajaya Mohan 2001). In Fig.

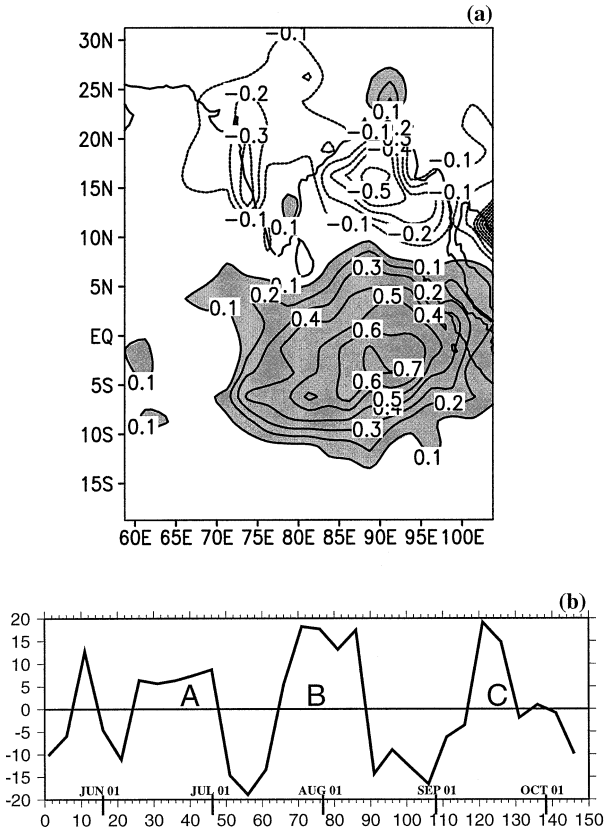

FIG. 4. (a) The spatial distribution of the first EOF component of rainfall calculated from the pentadal rainfall data for the 2000 monsoon season. Note that the intraseasonal variability is dominated by the pattern of rainfall anomaly having opposite polarities over the Indian landmass and the tropical Indian Ocean. (b) The pentadal time series of the first PC starting around 17 May 2000 and ending around 9 Oct 2000. The symbols (A, B, C) roughly coincide with the timing of the three major break spells during 2000.

1b, we had discussed the three major break spells that occurred during the 2000 monsoon season. Here, we present a quantitative assessment of the out-of-phase behavior of the intraseasonal convective anomalies over the subcontinent and the equatorial IO, for the 2000 monsoon season, by performing a principal component (PC) analysis of the CMAP pentadal rainfall anomalies. The PC/EOF technique involves expanding a space–time field in terms of linearly independent orthogonal basic functions. This analysis provides percentage contributions to the total variance explained by the different linearly independent components. The structure of the leading EOF in Fig. 4a shows a pattern of negative anomalies over the Arabian Sea, Indian land region, and the Bay of Bengal; and positive anomalies over the tropical southern IO. This first EOF pattern explains about 21% of the total variance. It is important to note that the independent contribution from the first EOF is not small in view of the fact that it accounts for variations over a large region that includes the subcontinent as well as the equatorial and southern tropical Indian Ocean (EQSIO). We have examined the other EOF components as well. The structure of the second EOF showed decreased rainfall over India; however, the increased rainfall over the equatorial IO associated with the second EOF was not as prominent as the first EOF (figure not shown). The second EOF accounted for about 14% of the total variance; while the individual contributions from the third and higher EOFs were less than 10%. The time series of the first PC (Fig. 4b) indicates three peaks (A, B, C), which are found to correspond well with the timing of the three major monsoon breaks. This result further substantiates that the monsoon breaks during 2000 were strongly linked to the fluctuations of intraseasonal convective activity over the tropical IO. It must be pointed out that the evolution of the pentadal rainfall anomalies during 2000 actually revealed northward and northwestward migration of anomalies from the equatorial Indian Ocean and Bay of Bengal towards north-central India (Krishnan et al. 2001). However, the impression of a standing oscillation may come from Fig. 4, possibly due to the amplitude modulation of the northward-propagating convective disturbance by an envelope whose primary maximum over the Indian subcontinent and secondary maximum over the equatorial and southern IO vary out of phase. Furthermore, using a power spectrum analysis, we have verified that the first PC time series shows spectral peaks around 15 and 45 days. These two timescales are reminiscent of the 10–20- and 30–60-day oscillations of the monsoon system described by earlier studies (Krishnamurti and Bhalme 1976; Dakshinamurti and Keshavamurty 1976; Yasunari 1979; Krishnamurti and Subrahmanyam 1982; Goswami and Ajaya Mohan 2001).

The striking asymmetry in the meridional out-of-phase pattern of the intraseasonal variability during 2000 can be illustrated from the rainfall and low-level wind anomalies associated with the break and active phases of the monsoon. The plot in Fig. 5a shows composites of pentadal anomalies for the three major break spells during 2000. The pattern of negative rainfall anomaly over the Indian land region and the positive anomaly over the equatorial IO resembles that of the first EOF. Such an out-of-phase pattern of convective anomalies over the two regions has been reported by previous studies (Yasunari 1979; Sikka and Gadgil 1980, Krishnan et al. 2000; Goswami and Ajaya Mohan 2001). The anomalous easterlies and the anticyclonic circulation to the north indicate a weakening of the monsoon flow; while the anomalous low-level convergence over the IO represents an intensification of the equatorial shear zone. The strengthening of the near-equatorial shear zone, commonly referred to as the Southern Hemispheric Equatorial Trough, seen in the break composite (Fig. 5a) has been long known in the Indian meteorological literature (De, it et al. 1997). The small region of increased rainfall over northeast India is a characteristic feature of breaks and is accompanied by a northward shift of the monsoon trough to the Himalayan

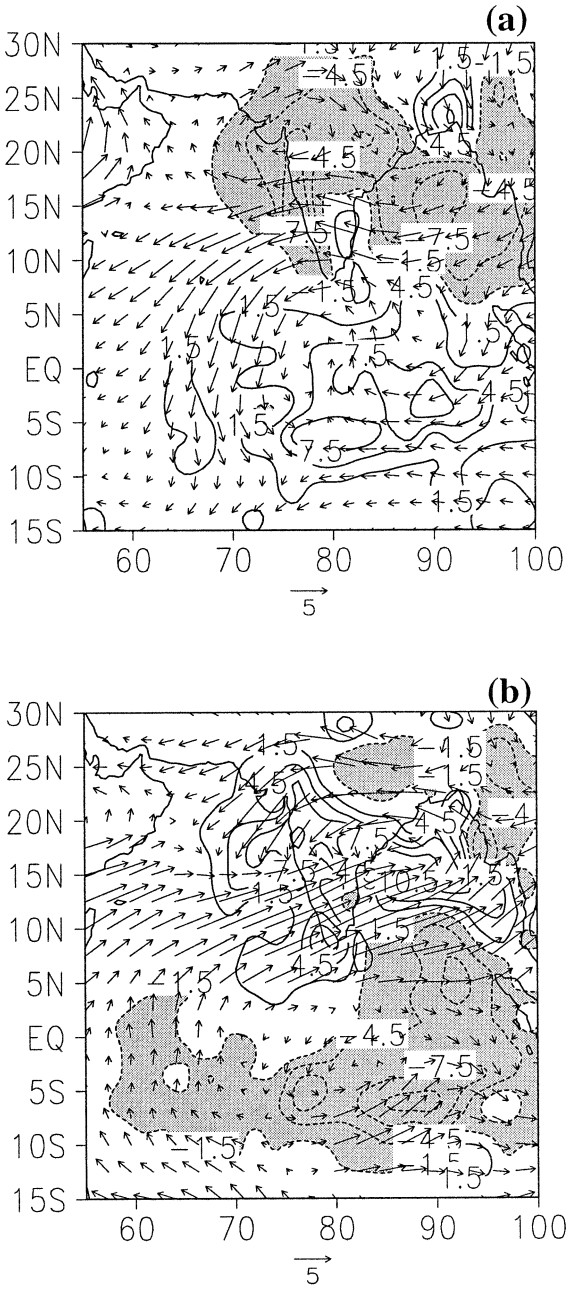

FIG. 5. Composite anomaly patterns of rainfall (mm day^{-1}) based on the pentadal CMAP data and 850-hPa winds (m s^{-1}) from NCEP reanalysis. (a) Break monsoon composite based on pentads centered around 19 Jun, 19–24–29 Jul, 3 Aug, 12–17 Sep 2000. (b) Active monsoon composite based on pentads centered around 4 Jun, 9 Jul, 18–23 Aug 2000.

foothills (Ramamurthy 1969; Dhar et al. 1984; Krishnamurthy and Shukla 2000). The anomaly pattern in Fig. 5b is a composite of the active monsoon spells during 2000. Note that the spatial structure of the anomaly in this case is nearly opposite to that of the break composite and clearly brings out the bimodal character of the monsoon intraseasonal variability. Furthermore, the meridional out-of-phase pattern appearing both in the seasonal mean anomaly (Fig. 3c) and the intraseasonal variability (Fig. 5a), provides a basis for the linear superposition of the ''active'' or ''break'' monsoon conditions to influence the seasonal mean monsoon rainfall for a particular year (Goswami and Ajaya Mohan 2001; Krishnamurthy and Shukla 2000). Detailed discussion on this aspect, which concerns the probability of occurrence of active and break conditions, will be taken up in section 3b.

c. Enhancement of convection over the equatorial Indian Ocean

The picture emerging from the PC/EOF analysis (Fig. 4) clearly demonstrates that the anomalous enhancement of convection over the warm tropical Indian Ocean was a predominant feature during the 2000 monsoon season. The effect of SST on deep convection must be realized through modification of the dynamic and thermodynamic conditions in the atmospheric boundary layer and above. There have been studies suggesting that SSTs in excess of 27.5°C *are necessary but not sufficient* for the occurrence of deep convection over tropical oceans (Gadgil et al. 1984; Graham and Barnett 1987). The results of Zhang (1993) indicate that the variability of deep convection becomes larger for higher SST. He argued that factors unfavorable to convection can sometimes be so dominant as to suppress upward vertical motions in spite of high SST. According to Graham and Barnett (1987), the divergence of the surface winds is an important agent in determining the presence or absence of convection over high SST regions. In interpreting the connection between SST and convection over the IO, we draw attention to the study by Lindzen and Nigam (1987) who proposed that in areas of maximum SST, the surface moisture convergence induced by large-scale SST gradients in the Tropics plays a crucial role in determining the distribution of convection and precipitation. They showed that SST as a boundary condition influences the moisture convergence at the surface, which together with fluxes of latent and sensible heat from the warm tropical oceans into the atmosphere, makes conditions more favorable for deep convection. Lindzen and Nigam (1987) particularly highlighted the importance of meridional gradients of SST in affecting the zonal winds over the tropical oceans. The thin line in Fig. 6a shows the latitudinal variation of climatological SST in the IO obtained by averaging the SST field zonally between (50°–100°E). Note that the SST maximum occurs in the equatorial latitudes (3°S–3°N). To the south of the equator the magnitude of SST drops off more rapidly. The SST decrease to the north of 3°N is in association with the evaporative cooling in the Arabian Sea and northern Indian Ocean by the southwest monsoon winds (Krishnamurti 1985). The latitudinal variation of SST during 2000 is shown by the thick line in Fig. 6a. The following are some of the noteworthy

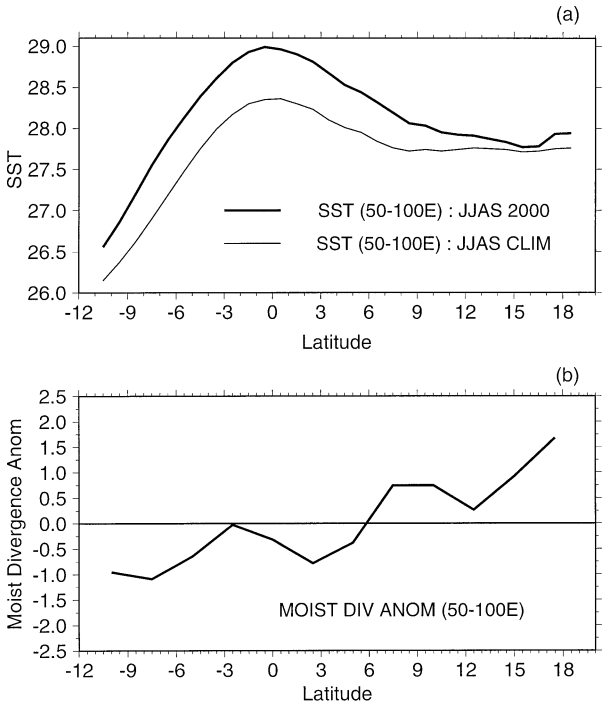

FIG. 6. The latitudinal variation of (a) SST (°C) during 2000 (thick line) and climatological SST (thin line) (b) Anomaly of $\nabla \cdot \mathbf{Q}$ for JJAS 2000 (1.0×10^{-6} kg m^{-2} s^{-1}). The SST and $\nabla \cdot \mathbf{Q}$ fields were averaged zonally between 50°–100°E.

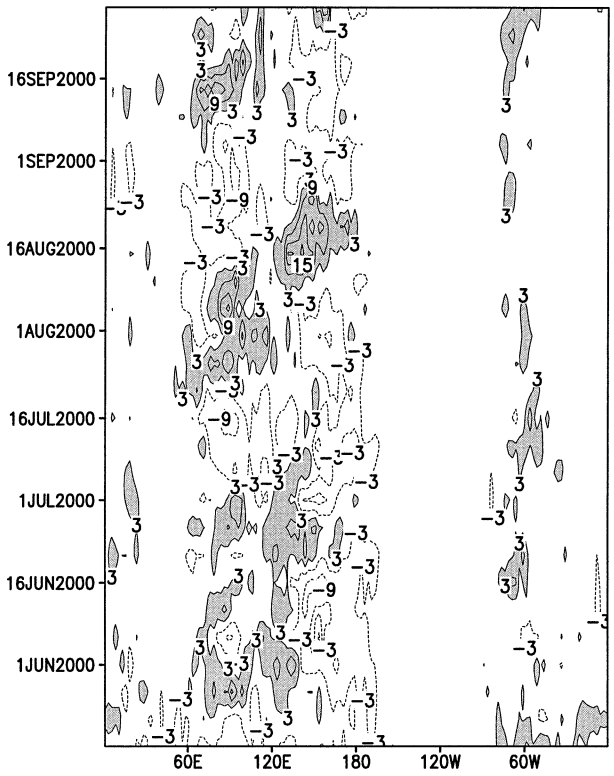

FIG. 7. The longitudinal variation of the CMAP pentadal rainfall (mm day^{-1}) anomalies during 2000. The anomalies were averaged between 5°N–5°S. Note that the equatorial intraseasonal oscillations are strongly confined over the Indian Ocean and the west Pacific sector.

aspects with regard to the meridional gradient of SST. The climatological SST curve has a maximum of about 28.4°C near the equator and drops to about 27.7°C around 15°N. On the other hand, the 2000 SST curve has a maximum of about 29°C at the equator and decreases to about 27.8°C around 15°N. Thus a steeper meridional gradient of SST can be noted during 2000 as compared to the climatology, with the equatorial IO being warmer than normal by about 0.6°C in 2000. Furthermore, the relatively warmer SST conditions to the north of the equator during 2000 is consistent with the decrease in evaporative cooling in the Arabian Sea due to the weakening of the low-level monsoon winds. It was earlier shown in Fig. 3c, that the monsoon 2000 anomaly patterns exhibited increased moisture convergence over the equatorial IO, but anomalous divergence over the Indian land region. The latitudinal variation of the anomalous moisture divergence term (Fig. 6b) indicates negative values around the equator, implying enhanced convergence at these latitudes; and positive values (anomalous divergence) to the north of 6°N. Thus the negative meridional gradient of SST (~ -1.2°C between the equator and 15°N) during 2000 and the north–south variation of the moisture convergence anomalies are in accordance with the Lindzen–Nigam hypothesis.

Given the enhanced moisture convergence of the background flow over the warm tropical IO, we now examine the evolution of transients over the equatorial region during the monsoon season of 2000. One of the most prominent global phenomenon on the subseasonal timescale is the tropical intraseasonal oscillation (ISO). The basic features of the ISO have been documented by numerous studies; a comprehensive review of the observational aspects of the ISO has been described by Madden and Julian (1994). To a first order, the ISO consists of eastward-propagating planetary-scale perturbations of atmospheric circulation with predominant wavenumbers 1 and 2. The largest amplitudes of the ISO occur over the Indian and western Pacific Oceans and the convective anomalies in this sector exhibit a slow eastward propagation having phase speed of about 5 m s^{-1} with the dominant periods of the ISO ranging from 30 to 60 days. The plot in Fig. 7 shows the longitude–time section of pentadal rainfall anomalies over the near-equatorial region during 2000. The rainfall anomalies were constructed by subtracting the smooth pentadal climatology from the CMAP rainfall for 2000. One can notice that the longitudinal band extending from the central IO up to the west Pacific Ocean (70°–130°E) in Fig. 7 is characterized by four major wet spells during June–September of 2000. The first enhanced rainfall spell over the equatorial oceans occurred during early June; the second during later half of June and early July; the third spell was a long one extending from the third week of July up to the second week of August;

the fourth spell started around the second week of September and lasted about 2 weeks or so. It should be pointed out that the second, third and fourth wet events over the equatorial sector approximately coincided with the three major break spells over the Indian land region. Further, it is important to notice in Fig. 7 that the equatorial rainfall anomalies were largely confined over the warm waters of the Indian and western Pacific Oceans, and had rather small amplitudes to the east of the dateline. Observational evidence indicates that the variability of convection associated with the ISO can be substantial over warm SST regions of the tropical Indian and western Pacific Oceans (Weickmann et al. 1985). Theoretical and modeling studies provide support for the intensification and slowing down of the eastward-propagating equatorial waves due to the effect of increased moisture convergence (Lau and Peng 1987; Wang 1988; Kasture et al. 1991; and several others). In the light of these discussions, it is quite likely that the intensified convection over the equatorial IO during the 2000 monsoon season might have been generated largely from a combined influence of increased large-scale moisture convergence over the warm ocean surface and the amplification of the transient convective activity associated with the ISO.

3. Model experiments

In this section, we will describe the GCM experiments that were performed in order to assess the atmospheric response to the SST forcing during 2000. We have carried out four sets of 10-member ensemble integrations using the COLA GCM. These ensemble runs involve integrating the GCM from ten different initial conditions and provide a means for assessing the robustness of the simulated response to a given boundary forcing. The need to consider such multiple realizations arises because model simulations of the seasonal mean monsoon are affected not only by slowly varying boundary conditions like SST but also by atmospheric internal dynamics (Brankovic and Palmer 1997; Mujumdar and Krishnan 2001). Thus, ensemble realizations obtained from the multiple runs of the GCM starting from different initial conditions enable the determination of estimates for statistical significance of the simulated anomalies. A summary of the SST boundary forcing and initial conditions used in our experiments is presented in Table 1. The ensemble runs were initiated from 10 different observed initial conditions (22–31 May 2000) from NCEP. All the model runs, starting from different initial conditions, go through 30 September 2000. We first processed the NCEP initial conditions containing the spectral coefficients of vorticity, divergence, temperature, moisture, and surface pressure so that they become compatible with the COLA T30L18 GCM. Subsequently these 10-member initial conditions were used to start the model runs in all four experiments. In the first set (CLIM) of ensemble experiments, we use the observed monthly climatological SSTs as boundary forcing for the GCM. The boundary forcing for the second set (GL2K), is obtained by superposing the observed monthly SST anomalies of 2000 upon the monthly SST climatology for the global oceans. In the third set (IO2K), we superpose the monthly SST anomalies of 2000 on the climatological SST only in the Indian Ocean (40°–120°E), while retaining climatological SSTs in all the other oceans. The meridional extent of the IO2K domain includes the 2000 SST anomalies for the entire IO extending from the Bay of Bengal, Arabian Sea, and the tropical and southern IO. The idea behind the IO2K experiment is to understand exclusively the influence of the IO SST anomalies on the atmosphere. In the fourth experiment (NOIO), we specify climatological SST in the IO (40°–120°E) domain and superpose the 2000 monthly SST anomalies on the climatology in all other oceans. Unlike the IO2K case, the NOIO experiment is intended to evaluate the influence of SST anomalies in all other oceans excepting the IO. The procedure adopted for evaluating the anomalous response to SST forcing is to compare the ensembles of the GL2K, IO2K, and NOIO simulations with those of the CLIM experiment. Since the four experiments have been initiated from identical sets of 10 observed initial conditions, it is possible to carry out a member-to-member comparison between the GL2K and CLIM, IO2K and CLIM, and NOIO and CLIM experiments. This approach provides a straightforward means for assessing the simulated response to SST forcing (Mujumdar and Krishnan 2001).

a. Simulated seasonal features

1) RAINFALL AND MOISTURE TRANSPORT

The ensemble mean of the seasonal rainfall and moisture transport vector simulated by the CLIM experiment is shown in Fig. 8a. The overall spatial distribution of the monsoon precipitation is reasonably captured by the GCM; the simulated water vapor transport by the southwest monsoon winds and the cross-equatorial flow is broadly consistent with that of the NCEP reanalysis. However, some of the finer details of monsoon rainfall are not as well simulated—maybe partly because of the coarse model resolution and partly due to deficiencies in the treatment of physical processes in the GCM. For instance, the west coast rainfall maximum over India is weak and is shifted more westward as compared to the CMAP precipitation. Also the rainfall maximum over the Bay of Bengal shows a southward shift relative to the observed position. While noting such discrepancies, we must also point out that a large number of the state-of-the-art GCMs face a big challenge in accurately simulating the monsoon rainfall distribution (Gadgil and Sajani 1998). Moreover, it is important to mention that the primary purpose of the GCM experiments is not to critically focus on the accuracy of the monsoon simu-

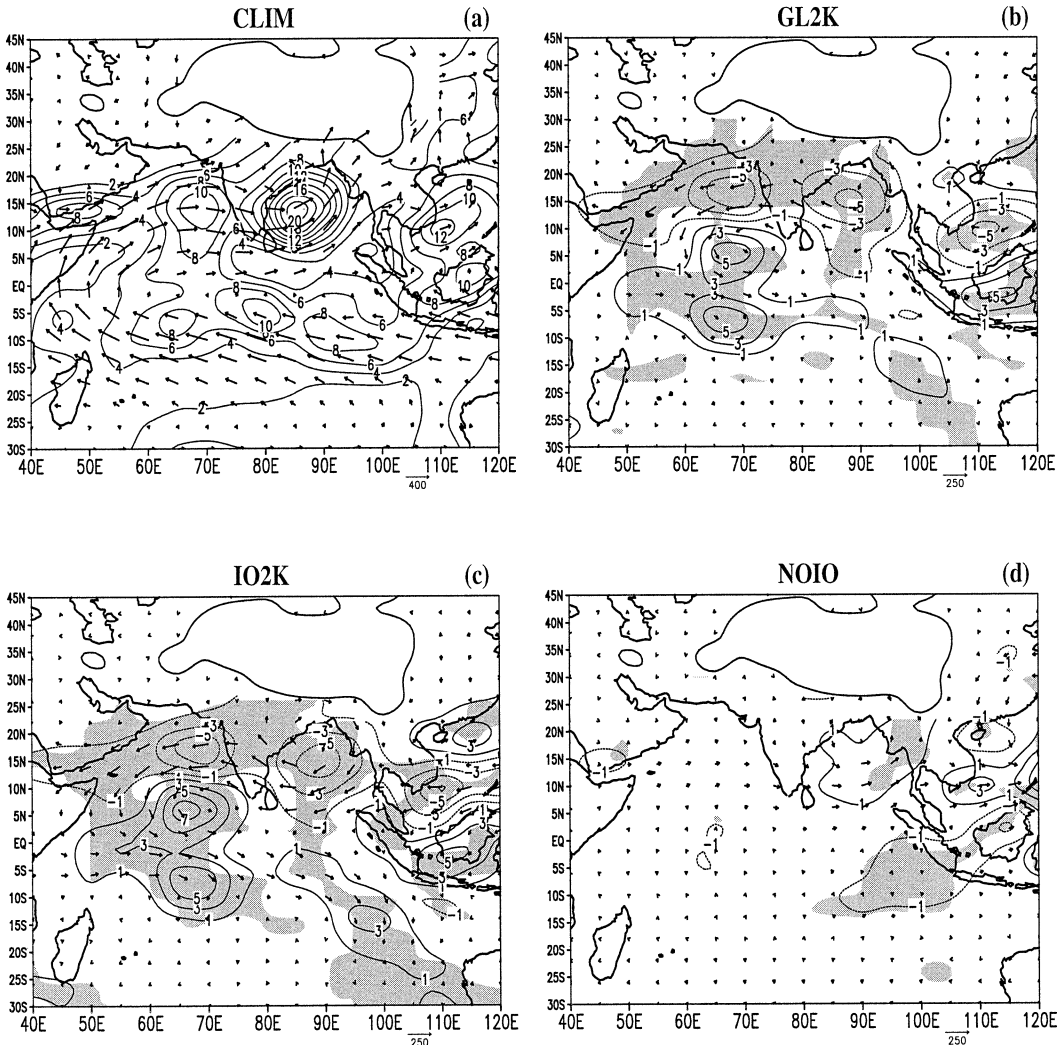

FIG. 8. (a) The GCM-simulated JJAS rainfall (with contour interval of 3 mm day^{-1}) and **Q** (kg m^{-1} s^{-1}) for the CLIM experiment. The fields shown are averages of the 10 ensemble realizations. (b) Same as in (a) except for the GL2K anomalies. (c) Same as in (a) except for the IO2K anomalies. (d) Same as in (a) except for the NOIO anomalies. Anomalies in (b)–(d) are obtained by taking averages of the member-to-member differences for GL2K and CLIM, IO2K and CLIM, and NOIO and CLIM, respectively; also, shaded areas correspond to areas where the simulated rainfall anomaly exceeded the 99% significance level computed from a *t* test.

lation; instead, the experiments are aimed at providing an overall picture of the large-scale character of the monsoon and its anomalous behavior during 2000.

We shall now examine the anomalous response to SST forcing in the GL2K experiment. For this reason, we compute the mean of the member-to-member differences between the GL2K and CLIM experiments. The statistical significance of the simulated anomalies has been evaluated by applying the classical *t* test (Mujumdar and Krishnan 2001). The anomaly pattern for the GL2K run in Fig. 8b, shows decreased rainfall and an anomalous anticyclone over the Indian subcontinent, Arabian Sea, and Bay of Bengal. The anomalous easterly flux over this region indicates a decrease in the transport of moisture into the Indian region, which qualitatively agrees with the NCEP anomalies (Fig. 3c). The response over the EQSIO shows increased rainfall and intensified circulation. The simulated anomalies over the IO are more westward as compared to CMAP and NCEP anomalies. This westward displacement of the simulated rainfall anomaly is in accord with the westward displacement of the CLIM precipitation in the model. In short, the north–south asymmetry in the rainfall and moisture transport anomalies is broadly consistent with the CMAP and NCEP datasets. Furthermore, the shaded area in Fig. 8b suggests that the contrasting rainfall anomalies over the Indian land and oceanic regions exceed the 99% level of statistical significance.

The precipitation and moisture transport anomalies for the IO2K experiment obtained from the ensemble

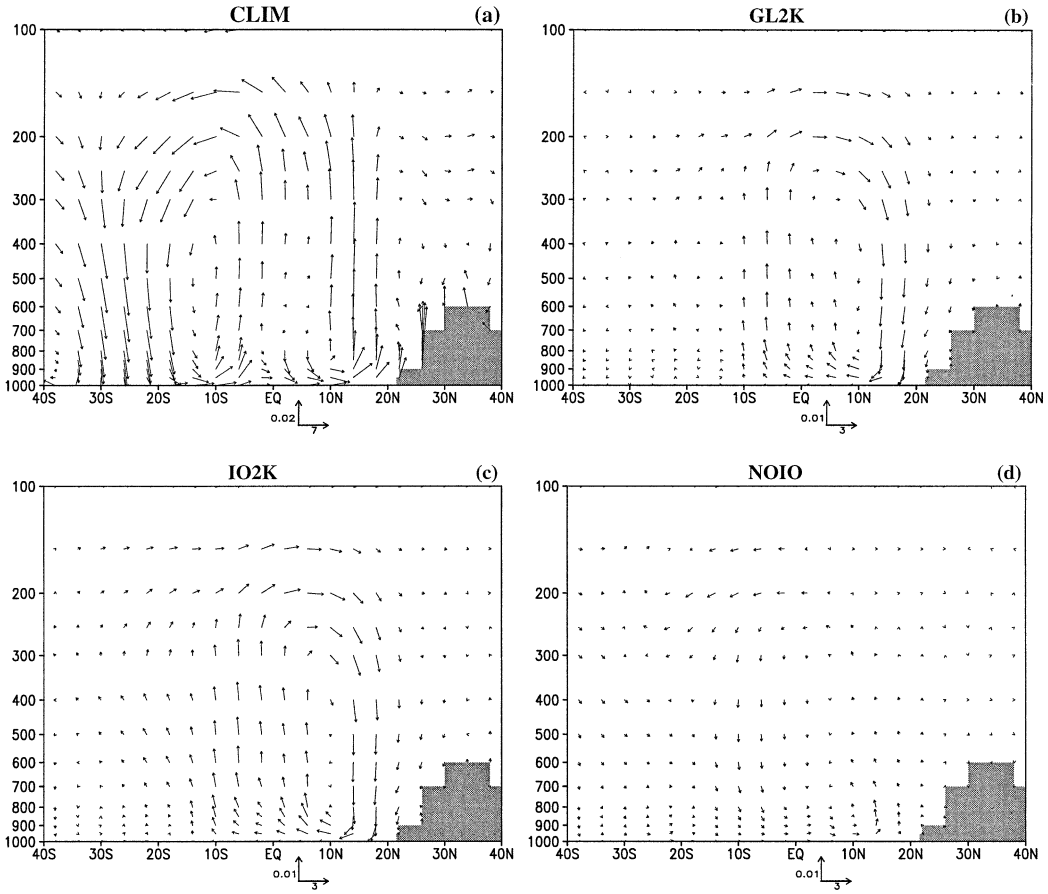

FIG. 9. (a) The simulated monsoon Hadley cell for JJAS in the CLIM experiment. The meridional wind (m s^{-1}) and vertical wind (hPa s^{-1}) components are averaged longitudinally between 50°–100°E. (b) Same as in (a) except for the GL2K anomalies. (c) Same as in (a) except for the IO2K anomalies. (d) Same as in (a) except for the NOIO anomalies.

mean of the member-to-member differences between the IO2K and CLIM runs, are shown in Fig. 8c. The anomalous response in the IO2K experiment closely resembles that of the GL2K experiment with regard to the asymmetric pattern of the rainfall and moisture transport anomalies. This points out that the impact due to the IO SST forcing, which was common to both the GL2K and IO2K runs, was dominant in the GCM simulated response. The *t* test for the IO2K simulation shows that the rainfall anomalies with opposite polarities over the Indian land and oceanic regions are statistically significant. Thus the simulations indicate that the influence of the IO SST forcing was largely responsible for the observed seasonal anomaly during 2000. This basically supports the concept that the presence of warm SST anomalies in the tropical IO tends to decrease the seasonal monsoon rainfall over India, as noted by earlier studies (e.g., Chandrasekar and Kitoh 1998). The simulated precipitation and moisture transport anomalies in the NOIO experiment (Fig. 8d) are insignificant over most of the region. The small negative values of rainfall anomalies over the eastern southern IO seem to be associated with the response due to the SST anomalies in the tropical west Pacific Ocean. Here, it is important to mention the sensitivity of the COLA GCM to remote SST forcing in the tropical Pacific. In a recent study, Kirtman and Shukla (2001) have analyzed results from a 50-yr (1949–98) run of the COLA GCM forced with observed SST, and examined the ENSO–monsoon relationship as simulated by the GCM. They noted that the GCM simulated monsoon rainfall is unable to reproduce the observed ENSO–monsoon relationship. Therefore, while the monsoon rainfall anomalies in the NOIO simulation (Fig. 8d) appear to be rather insensitive to the weak negative SST anomalies in the tropical central-eastern Pacific Ocean during 2000, it is also realized that the NOIO experiment could have been partly affected by the model's systematic errors.

2) MONSOON HADLEY CIRCULATION

The simulated overturning in the *y–p* plane for the CLIM experiment (Fig. 9a) is qualitatively consistent with the NCEP reanalysis in capturing the monsoon

Hadley cell with an ascending branch to the north of 15°N and a descending motion over the southern IO. The *y–p* circulation anomaly in the GL2K simulation (Fig. 9b) shows a weakening of the Hadley cell characterized by anomalous sinking around 15°–20°N and anomalous rising motion around 0°–10°S over the tropical IO. Note that the anomalous sinking in the GL2K experiment is seen mainly to the north over the subcontinent. However the observed anomalous subsidence over the subtropical southern IO is absent in the GL2K response. Thus, while the model simulates the weakening of the monsoon Hadley cell, it fails to realistically capture the Hadley circulation anomalies over the Southern Hemisphere. It may also be noted that the GL2K simulation does not reveal the observed negative precipitation anomalies to the south of the near-equatorial positive rainfall anomaly. The explanation for this model bias is not clear and will require detailed examination of the treatment of moist convection in the GCM and its dependency on atmospheric thermodynamics and SST boundary forcing. The anomalous weakening of the monsoon Hadley cell in the IO2K experiment (Fig. 9c) is strikingly similar to that of GL2K run. Note that the circulation anomaly in GL2K and IO2K experiments appear to be more pronounced than that of the NCEP reanalysis, suggestive of the strong sensitivity of the GCM response to the IO SST forcing. On the other hand, the monsoon Hadley cell anomaly for the NOIO experiment (Fig. 9d) is almost negligible.

b. Simulation of monsoon breaks

The conceptual model for the intraseasonal oscillations of the monsoon system proposed by Krishnamurti and Bhalme (1976) involves interactions among dynamics, moist convection, and cloud-radiative processes. The question that now arises is about the external influence of SST forcing on the monsoon intraseasonal oscillations. In the context of the 2000 monsoon, we shall specially examine the role of the tropical IO SST anomalies in altering the regional intraseasonal convective anomalies. For this purpose, we have analyzed the GCM simulated outputs of daily rainfall anomalies from the different experiments. The rainfall anomalies in the GCM were computed relative to daily normals prepared by averaging the rainfall output from a large number of CLIM SST runs initiated from different initial conditions (see text of Fig. 10a). The time series of the daily normal rainfall for the GCM, averaged over the Indian region, is shown in Fig. 10a. It can be seen that a large part of the monsoon rainfall in the model occurs during July and August. The low rainfall in the beginning and end periods of the integrations are associated with model spinup and early withdrawal of the monsoon, respectively, which should not impact the thrust of this analysis (Mujumdar and Krishnan 2001). In interpreting the GCM-simulated intraseasonal variability, it is important to point out that the day-to-day evolution of the monsoon rainfall in different ensemble realizations is sensitive to the atmospheric internal dynamics and the choice of initial conditions. In other words, the phase, amplitude, and frequency of intraseasonal variability can considerably differ from one member to another, even if the SST boundary forcing is fixed (Brankovic and Palmer 1997). Therefore, it is meaningful to evaluate the statistics of the GCM-simulated intraseasonal variability, rather than directly compare the daily transients from the different GCM ensemble realizations with observations.

Having prepared the daily rainfall normals and the daily anomalies for all the members of the different GCM experiments, we shall now describe the procedure through which the break days have been objectively determined from the GCM simulations. The criterion we have devised in selecting the monsoon break days is that the percentage departure of the area-averaged (10°–30°N; 70°–95°E) rainfall from the normal should be below 30% for at least 5 consecutive days. In adopting the above definition, we keep in mind the broad spatial pattern of observed rainfall departures during breaks, which typically varies from about −25% over a wide area of central India up to about −75% over the drier regions of northwest India (Ramamurthy 1969). Before proceeding further, we shall use the example of the time series in Fig. 10b and the anomaly maps in Figs. 10c–e to illustrate clearly the evidence for the GCM-simulated intraseasonal variability and the break identification procedure. The example in Fig. 10b is the time series of daily rainfall departures of the area-averaged rainfall for one of the members of the GL2K experiment. The shaded bars in Fig. 10b are the break days, which satisfy the criterion described earlier. The fact that these simulated negative rainfall departures (less than −30% of the normal) over a large area persist for more than 5 days indicates that the breaks identified in the GCM simulations are linked with intraseasonal variability. This particular example happens to have three break spells (17–30 June, 11–16 July, 26 July–17 August). However, in general the active/break spells can vary considerably from one member to another, because of the sensitivity of the evolution of GCM intraseasonal transients to atmospheric internal dynamics and the choice of the initial conditions. The total number of break days in this example is 43. Note that the GL2K experiment uses the warm SST boundary condition of 2000 and it can be seen that the day-to-day monsoon rainfall variations in this example are predominantly below normal. Anomaly maps of rainfall and low-level winds associated with the three break spells from the GL2K example are shown in Figs. 10c–e. Note that the three break spells in this example are associated with a widespread decrease of rainfall over the subcontinent, Bay of Bengal, and the Arabian Sea; and accompanied by low-level anticyclonic wind anomalies in the region. Furthermore, the pattern of decreased rainfall over the

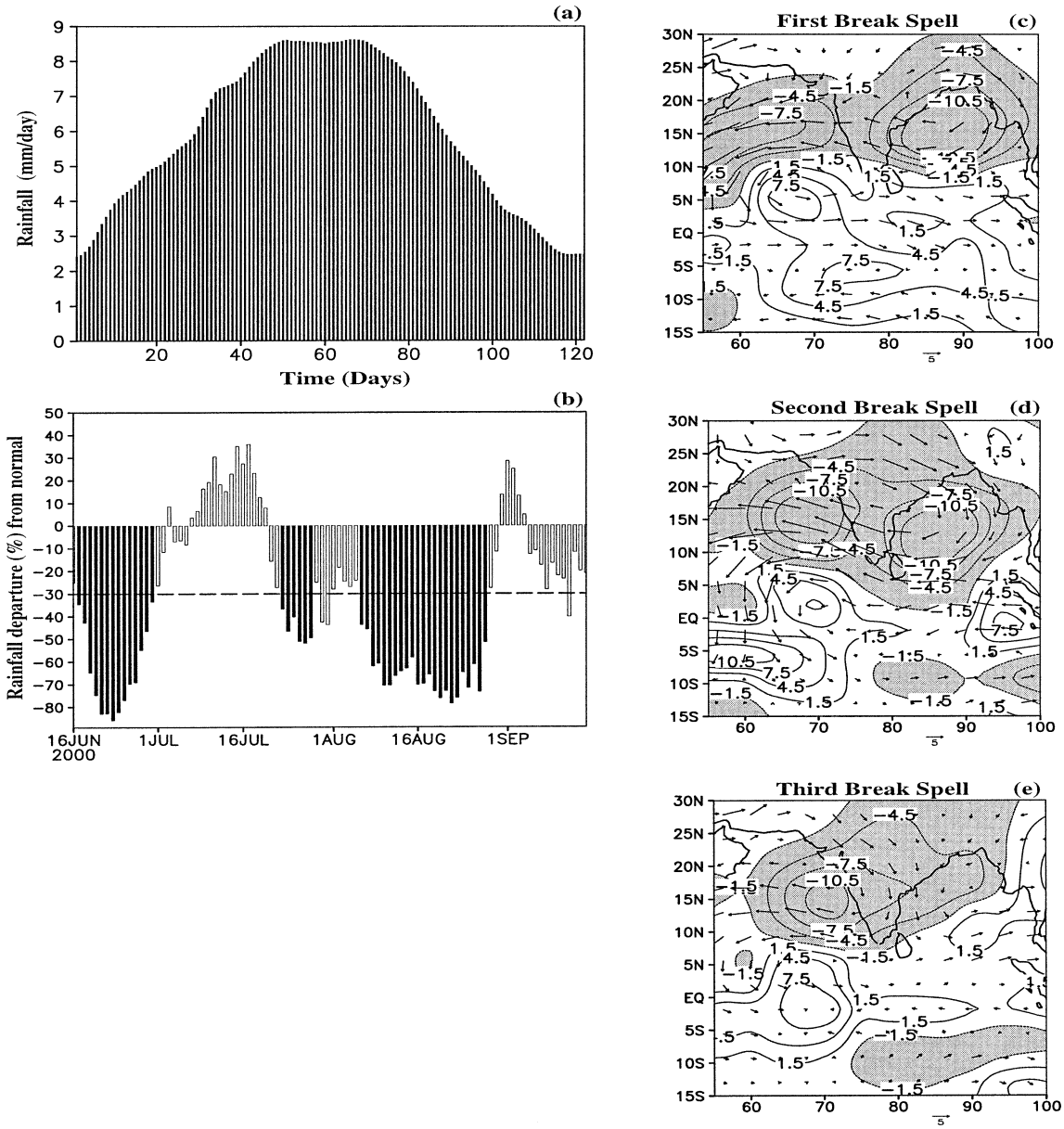

FIG. 10. (a) Time series of daily rainfall normals averaged over 10°–30°N, 70°–95°E for the COLA GCM from 1 Jun to 30 Sep. This time series is a mean of daily rainfall from 30 cases of CLIM SST runs that were initiated from 30 different atmospheric initial conditions (10 members each year during 2000, May 1987, and May 1988). A 3-day running mean is applied on the daily rainfall normals. (b) Example illustrating the time series of daily rainfall departures over the Indian region from one of the GL2K members during the core monsoon season (15 Jun–15 Sep). The dashed line corresponds to the −30% rainfall departure from normal. The dark-shaded bars are the break days identified using the criterion that the percentage departure of the area-averaged rainfall from the normal should be below 30% for at least 5 consecutive days. (c) Rainfall (mm day^{-1}) and 850-hPa wind (m s^{-1}) anomalies associated with the first break spell of the GL2K example. (d) Same as in (c) except for the second break spell. (e) Same as in (c) except for the third break spell.

Indian subcontinent and increased rainfall over the EQSIO is seen consistently in all three break spells of the GL2K example. Thus the widespread nature of the rainfall and wind anomalies in Figs. 10c–e provides additional support for the large-scale structure of the break-monsoon anomalies simulated by the GCM.

By applying the break identification procedure successively to all the 10 ensemble members for any given experiment (say GL2K), we collect all the break cases from all the different realizations of any given experiment. Later the composite is calculated by averaging the anomaly patterns over all the collected break days, from the 10 different realizations, of any given experiment. This process of making break composites is applied to the CLIM, GL2K, IO2K, and NOIO experiments. The idea behind making composites is to get an

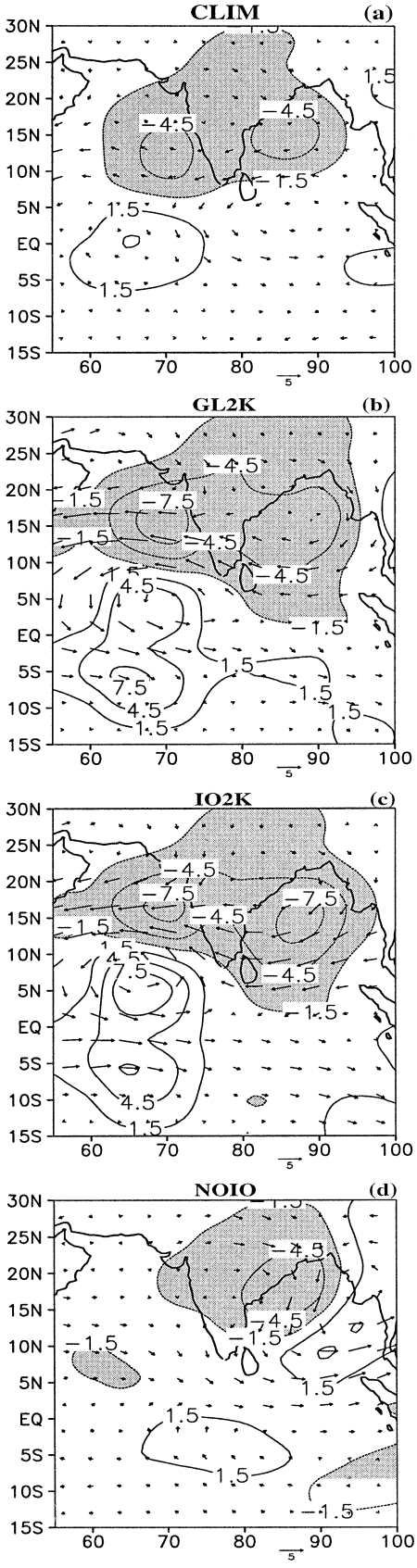

average picture of how break anomaly patterns appear in each of the four ensemble experiments. The break anomaly composites of rainfall and low-level circulation anomalies for the CLIM, GL2K, IO2K, and NOIO experiments are shown in Figs. 11a,b,c,d respectively. The composite in the CLIM experiment shows a pattern of decreased rainfall and low-level anticyclonic anomaly over India, the Arabian Sea, and the Bay of Bengal. A slight increase in the precipitation is seen over the southern side of the equatorial IO. The SST boundary condition in the CLIM experiment contains only the seasonally varying climatological component. Hence, the break composite for the CLIM experiment basically reflects the rainfall decrease resulting from atmospheric internal dynamics and does not contain the influence of SST anomalies. On the other hand, the break anomalies for the GL2K and IO2K experiments include contributions both from atmospheric internal dynamics as well as the SST anomalies of 2000. One can see that the break monsoon anomalies in GL2K and IO2K appear to be more intense with a wider spread as compared to the CLIM runs. Particularly, the rainfall increase over the EQSIO and the anomalous intensification of the near-equatorial shear zone is more pronounced in the GL2K and IO2K experiments. The meridional out-of-phase structure of the break anomalies in the GL2K and IO2K cases has similarities with the corresponding seasonal anomalies in Figs. 8b,c, suggesting that the enhanced break condition could have led to the decrease in the simulated seasonal mean monsoon rainfall during 2000. According to Goswami and Ajaya Mohan (2001), the similarities in the spatial structures of the seasonal mean anomaly and the intraseasonal variability provides a basis for the linear superposition of the active or break monsoon conditions to influence the seasonal mean monsoon rainfall for a particular year. This point will be discussed in the next section. We do recognize the limitations of the GL2K and IO2K simulations with respect to the observed pattern of break monsoon anomaly. For instance, it is seen that the simulated rainfall anomaly over the tropical southern IO is shifted more westward as compared to the observed break pattern (Fig. 5a). Also the GCM does not adequately capture the larger eastward spread of the negative rainfall anomalies to the north, which is seen in the observed break composite. Despite these differences, the GL2K and IO2K simulations are overall consistent with observations in indicating the reinforcement of the north–south asymmetric structure of break monsoon rainfall anomaly, which is suggestive of the effect induced by the SST anomalies during 2000. The break composite for the NOIO experiment (Fig. 11f) shows negative rainfall

←

FIG. 11. Composite anomaly maps of rainfall (mm day^{-1}) and 850-hPa winds (m s^{-1}) during monsoon breaks as simulated by the GCM experiments: (a) CLIM, (b) GL2K, (c) IO2K, (d) NOIO.

anomalies over India and the northern Bay of Bengal. The spatial extent of the negative rainfall anomaly over the Indian region is relatively small in the NOIO experiment as compared to the GL2K and IO2K experiments. Also the rainfall increase over the equatorial IO is marginal in the NOIO experiment. Although both the CLIM and NOIO experiments make use of climatological SST in the IO, the latter differs from the former by including the 2000 SST anomalies for the rest of the oceans. The consequence of such differences in the SST boundary conditions in the two experiments may be partly reflected in some of the regional differences in the break composites of the NOIO and CLIM experiments. For instance, the pattern of decreased rainfall extends more westward into the Arabian Sea in the CLIM run as compared to NOIO. Likewise, the increased rainfall to the south of the equator appears to be shifted more westward in the CLIM case as compared to NOIO. Nevertheless, both the CLIM and NOIO experiments share a common feature of showing a relatively weaker north–south asymmetric pattern of rainfall anomalies as compared to the GL2K and IO2K experiments.

1) Frequency distribution of daily rainfall anomalies

It is recognized that the mean summer rainfall over India during a particular year is substantially influenced by the probability of occurrence of wet/dry spells associated with the monsoon intraseasonal variability (Goswami and Ajaya Mohan 2001). From the viewpoint of interpreting the seasonal rainfall anomalies during 2000, we shall now consider the plot in Fig. 12a that shows the frequency distribution of the daily rainfall anomalies, for 122 days (1 June–30 September 2000), over the Indian subcontinent and the EQSIO region. The daily rainfall anomalies are based on the NCEP reanalysis dataset. Note that the CMAP dataset provides 5-day averages, while the NCEP rainfall is available on a daily basis. By organizing the rainfall departures into categories (or classes), we have determined the number of days belonging to each category having a bin size of 15%. The frequency distribution does not change significantly, if the bin size is changed. It can be seen from Fig. 12a that the distribution for the Indian subcontinent has a bimodal structure with a primary peak around −30% and a secondary peak around +30%. However, the more important point is that the frequency peak corresponding to the negative rainfall departure is higher in magnitude than that of the positive departure, indicating the predominance of monsoon break spells over the subcontinent during 2000. This higher probability of occurrence of monsoon breaks provides a consistent explanation for the below normal seasonal rainfall anomaly over the subcontinent. On the other hand, the frequency distribution for the EQSIO region shows a peak corresponding to a positive departure around

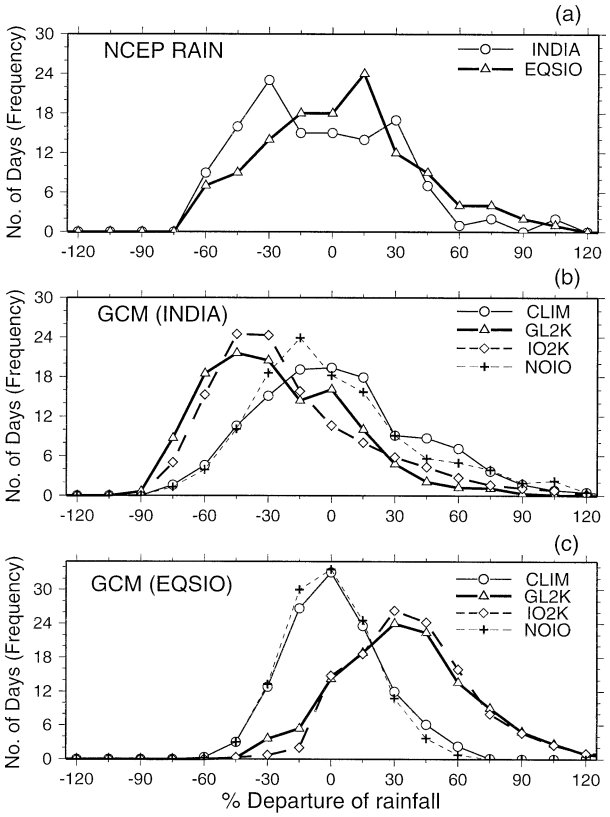

FIG. 12. Frequency distribution of daily rainfall departures for 122 days (1 Jun–30 Sep 2000). The rainfall departures are binned into categories having bin size 15%. (a) Rainfall departures based on NCEP reanalysis dataset. The thin line is for the Indian monsoon region (10°–25°N; 70°–90°E); the thick line is for the EQSIO (10°S–5°N; 75°–105°E). The choice of these two regions is based on the observed anomaly patterns with meridional out-of-phase structure (see Fig. 5). (b) Computed using the GCM outputs for the CLIM, GL2K, IO2K, and NOIO experiments for the Indian monsoon region (10°–30°N; 70°–95°E). Each curve is an averaged distribution from the 10 ensemble members. (c) Same as in (b) except for EQSIO region (10°S–5°N; 60°–90°E). Note that the GCM-simulated rainfall over the EQSIO region is shifted more westward relative to observations.

+15% indicating that this region was associated with higher frequency of enhanced rainfall during 2000. Clearly the two distributions in Fig. 12a bring out the contrasting nature of rainfall variability over the two regions.

The plot in Fig. 12b shows the frequency distribution of rainfall departures over the monsoon region simulated by the four sets of ensemble experiments. In computing the above statistics, we have utilized the outputs of daily rainfall from the different ensemble members of the four experiments. The four curves in Fig. 12b are averages of distributions from the 10 ensemble realizations of the CLIM, GL2K, IO2K, and NOIO experiments, respectively. It can be seen that the CLIM distribution is centered around zero. The shape of the CLIM distribution on either side of the maximum is nearly the same. On the other hand, the GL2K and IO2K distributions have

maxima centered around −45% and the skewness of the two curves indicates higher probability of occurrence of breaks for the GL2K and IO2K cases. Note that the maximum frequency of the GL2K and IO2K distributions are about 20 and 24 days, respectively. This suggests that on average, the GL2K and IO2K experiments showed at least 20 days (within a season) during which the rainfall was deficient by −45%. While the maximum for the NOIO distribution appears to be slightly on the negative side of the abscissa, the skewness is not clearly apparent in this case. Moreover it may be noted that the shape of the NOIO curve is more or less similar for both the positive and negative departures. Thus the frequency curves suggest that the intraseasonal variations of monsoon rainfall in the GL2K and IO2K runs were significantly inclined towards break spells as compared to the CLIM and NOIO cases. We have also confirmed that the total count of break days during the monsoon season were generally more in number in the GL2K and IO2K runs relative to the CLIM and NOIO ensembles. We realize that the GL2K and IO2K distributions do not show the observed secondary peak on the positive side. This appears to be related to the strong sensitivity of the GCM to anomalous SST forcing in GL2K and IO2K runs, so that the GCM considerably enhances the rainfall over EQSIO and induces strong subsidence over the subcontinent. Frequency distributions of the simulated rainfall departures over the EQSIO region are shown in Fig. 12c. It is interesting to note that the CLIM and NOIO distributions have a Gaussian-like shape and do not possess skewness. On the other hand, the GL2K and IO2K distributions show peaks corresponding to positive departures around +30%. These findings conclusively establish that the positive SST anomaly in the EQSIO region was responsible for causing enhanced and longer spells of convective activity in the equatorial region, which in turn induced prolonged breaks over the subcontinent. Thus it provides an explanation about the role of the IO SST anomaly in sustaining the meridional out-of-phase structure of the seasonal anomalies during 2000. It must be emphasized that an in-depth exploration of the physical mechanisms that couple SST, deep convection, and the large-scale monsoon dynamics, will be necessary in order to unravel the intriguing peculiarities of convection variability over the monsoon region.

Apart from the droughtlike monsoon of 2000, there have been other instances of dry monsoons (eg., 1979, 1986, 1987, 1995) in the past, which were associated with warm SST anomalies in the tropical IO (Krishnan et al. 2001). Some of them have occurred in conjuction with El Niño events in the Pacific Ocean. Likewise, there is also evidence of strong monsoon years (like 1961, 1994) that have coincided with SST cooling events in the southeastern Indian Ocean (Behera et al. 1999; Saji et al. 1999). It has been suggested by Behera et al. (1999), that evaporative cooling is one of key processes that can maintain the cold SST anomalies off the Sumatran coast; while the enhanced moisture transport from this region is important for sustaining the monsoon convection over the subcontinent. Recent studies have also drawn attention to the possibility of atmosphere–ocean coupling in the tropical Indian Ocean that is analogous to the Pacific ENSO (Webster et al. 1999; Saji et al. 1999). Nevertheless, the point that the IO SST anomalies in certain years can exert considerable influence on the seasonal mean monsoon raises an important question as to whether the IO SST boundary forcing is a much larger player in contributing to the interannual variability of the monsoon than perceived before.

4. Concluding remarks

Regional aspects of convection variability over the monsoon region and their association with the local SST forcing have not been fully understood yet. The circumstances that prevailed in the summer of 2000 provided an extraordinary opportunity to focus on this issue. During this season, the monsoon rainfall over the subcontinent was significantly suppressed; on the other hand, the EQSIO was characterized by positive SST anomalies and enhanced precipitation overlying the warm ocean surface. The dynamical fields revealed weakening of the monsoon Hadley cell; while increased moisture convergence and anomalous ascending motions occurred over the EQSIO. These anomalous features were accompanied by coherent intraseasonal fluctuations of regional convection. The subseasonal variability was dominated by prolonged breaks in the monsoon rainfall over the plains of India; and longer spells of increased convective activity over the EQSIO. The spatial structure of the leading EOF of intraseasonal rainfall variability, which explained about 21% of the total rainfall variance, exhibited a strikingly asymmetric north–south pattern of decreased precipitation over the Indian subcontinent; but increased precipitation over the EQSIO. In addition, the timing of the monsoon breaks over India was found to match well with the time series of the leading PC. All these results, when juxtaposed together, confirm that the sustenance of the subseasonal convective activity over the region of the southern equatorial trough was one of the pivotal factors that altered the monsoon large-scale circulation and the rainfall distribution during 2000.

Given that the seasonal mean monsoon rainfall in a particular year is closely linked to the probability of occurrence of the intraseasonal active/break spells (Goswami and Ajaya Mohan 2001), it is not obvious how the two timescales might have responded to the warm EQSIO SST anomalies during 2000. The GCM simulations for the GL2K and IO2K cases, which included the 2000 IO SST anomalies in the boundary conditions, were consistent in capturing the anomalous weakening of the monsoon Hadley cell and the precipitation decrease over the subcontinent; as well as the rainfall enhancement over the EQSIO. The decrease in the mon-

soon rainfall over the subcontinent, in response to the warm EQSIO SST anomalies, complements the idealized GCM simulations of Chandrasekar and Kitoh (1998). However, the more conclusive result emerging from our study is the point that the IO SST anomalies altered the regional intraseasonal variability in such a manner as to influence the seasonal mean monsoon during 2000. First, it is seen that the GCM results yield consistent support for the reinforcement of the meridional out-of-phase pattern of break monsoon rainfall anomaly, in response to the forcing by the warm IO SST anomalies. The spatial structures of the break anomaly pattern and the seasonal mean monsoon anomaly in the GL2K and IO2K experiments are found to be rather similar. In addition, it is shown that in the presence of the warm IO SST anomalies, the GCM simulations favored higher probability of occurrence of increased rainfall activity over the EQSIO, which in turn induced prolonged monsoon breaks leading to subdued rainfall over the subcontinent. These results, in short, establish the connection between the IO SST anomalies and the seasonal mean monsoon rainfall anomaly through the meridional out-of-phase structure of the monsoon intraseasonal variability. The present findings when viewed in the context that the IO SST anomalies in certain years can exert considerable influence on the seasonal mean monsoon, raises an important question as to whether the IO SST boundary forcing plays an active role in contributing to the monsoon interannual variability? Further studies will be necessary in order to address this question.

Acknowledgments. The authors thank the Director, Indian Institute of Tropical Meteorology, Pune, for providing the necessary facilities to carry out this work. This study was partly supported by the funds from the INDO-MOD/DOD project. Comments by the two anonymous referees led to considerable improvement of the manuscript and we gratefully acknowledge their helpful reviews. We also acknowledge the support extended by IITM, IMD, NCEP, NOAA, and CPC by making available to us the various datasets. We are very thankful to Drs. J. Shukla and Mike Fennessy for providing the COLA GCM. Finally, thanks are due to Dr. Rupa Kumar for scientific input.

REFERENCES

Barlow, M., H. Cullen, and B. Lyon, 2002: Drought in central and southwest Asia: La Niña, the warm pool, and Indian Ocean precipitation. *J. Climate,* **15,** 697–700.

Behera, S. K., R. Krishnan, and T. Yamagata, 1999: Unusual ocean-atmosphere conditions in the tropical Indian Ocean during 1994. *Geophys. Res. Lett.,* **26,** 3001–3004.

Brankovic, C., and T. N. Palmer, 1997: Atmospheric seasonal predictability and estimates of ensemble size. *Mon. Wea. Rev.,* **125,** 859–874.

Chandrasekar, A., and A. Kitoh, 1998: Impact of localized sea surface temperature anomalies over the equatorial Indian Ocean on the Indian summer monsoon. *J. Meteor. Soc. Japan,* **76,** 841–853.

Dakshinamurti, J., and R. N. Keshavamurty, 1976: On oscillation of period around one month in the Indian summer monsoon. *Indian J. Meteor. Geophys.,* **27,** 201–203.

Dhar, O. N., M. K. Soman, and S. S. Mulye, 1984: Rainfall over the southern slopes of the Himalayas and the adjoining plains during breaks in the monsoon. *J. Climatol.,* **4,** 671–676.

Fennessy, M. J., and Coauthors, 1994: The simulated Indian monsoon: A GCM sensitivity study. *J. Climate,* **7,** 33–43.

Gadgil, S., P. V. Joseph, and N. V. Joshi, 1984: Ocean-atmosphere coupling over monsoon region. *Nature,* **312,** 141–143.

——, and S. Sajani, 1998: Monsoon precipitation in the AMIP runs. *Climate Dyn.,* **14,** 659–689.

Goswami, B. N., and R. S. Ajaya Mohan, 2001: Intraseasonal oscillation and interannual variability of the Indian summer monsoon. *J. Climate,* **14,** 1180–1198.

Graham, N. E., and T. P. Barnett, 1987: Sea surface temperature, surface wind divergence and convection over tropical oceans. *Science,* **238,** 657–659.

Kalnay, E., and Coauthors, 1996: The NCEP/NCAR 40-Year Reanalysis Project. *Bull. Amer. Meteor. Soc.,* **77,** 437–471.

Kasture, S. V., V. Satyan, and R. N. Keshavamurty, 1991: A model study of the 30–50 day oscillation in the tropical atmosphere. *Mausam,* **42,** 241–248.

Kinter, J. L., III, D. G. DeWitt, P. A. Dirmeyer, M. J. Fennessy, B. P. Kirtman, L. Marx, E. K. Schneider, J. Shukla, and D. Straus, 1997: The COLA atmosphere–biosphere general circulation model. Volume 1: Formulation, COLA Tech. Rep. 51, Center for Ocean–Land–Atmosphere Studies, 46 pp.

Kirtman, B. P., and J. Shukla, 2000: Influence of the Indian summer monsoon on ENSO. *Quart. J. Roy. Meteor. Soc.,* **126,** 213–239.

——, and ——, 2001: Interactive coupled ensemble: A new coupling strategy for CGCMs. COLA Tech. Rep. 105, Center for Ocean–Land–Atmosphere Studies, 24 pp.

Krishnamurti, T. N., 1985: Summer monsoon experiment: A review. *Mon. Wea. Rev.,* **113,** 1590–1626.

——, 1986: Monsoon models. *Monsoons,* J. S. Fein and P. L. Stephens, Eds., John Wiley and Sons, 467–522.

——, and H. H. Bhalme, 1976: Oscillation of a monsoon system. Part I: Observational aspects. *J. Atmos. Sci.,* **33,** 1937–1954.

——, and D. Subrahmanyam, 1982: The 30–50 day mode at 850 mb during MONEX. *J. Atmos. Sci.,* **39,** 2088–2095.

Krishnamurthy, V., and J. Shukla, 2000: Intraseasonal and interannual variability of rainfall over India. *J. Climate,* **13,** 4366–4377.

Krishnan, R., C. Venkatesan, and R. N. Keshavamurty, 1998: Dynamics of upper tropospheric stationary wave anomalies induced by ENSO during the northern summer: A GCM study. *Proc. Indian Acad. Sci. (Earth Planet. Sci.),* **107,** 65–90.

——, C. Zhang, and M. Sugi, 2000: Dynamics of breaks in the Indian summer monsoon. *J. Atmos. Sci.,* **57,** 1354–1372.

——, M. Mujumdar, V. Vaidya, K. V. Ramesh, and V. Satyan, 2001: Modelling studies of the 2000 Indian summer monsoon and extended analysis. IITM Research Rep. 91, Indian Institute of Tropical Meteorology, Pune, India, 35 pp.

Lau, K.-M., and L. Peng, 1987: Origin of low frequency (intraseasonal) oscillations in the tropical atmosphere. Part I: The basic theory. *J. Atmos. Sci.,* **44,** 950–972.

Lindzen, R. S., and S. Nigam, 1987: On the role of sea surface temperature gradients in forcing low-level winds and convergence in the Tropics. *J. Atmos. Sci.,* **44,** 2418–2436.

Madden, R. A., and P. R. Julian, 1994: Observations of the 40–50-day tropical oscillations—A review. *Mon. Wea. Rev.,* **122,** 814–837.

Mujumdar, M., and R. Krishnan, 2001: Ensemble GCM simulation of the contrasting Indian summer monsoons of 1987 and 1988. IITM Research Rep. 89, Indian Institute of Tropical Meteorology, Pune, India, 33 pp.

Palmer, T. N., C. Brankovic, P. Viterbo, and M. J. Miller, 1992: Modeling interannual variations of summer monsoons. *J. Climate,* **5,** 399–417.

Pant, G. B., and B. Parthasarathy, 1981: Some aspects of an asso-

ciation between the Southern Oscillation and Indian summer monsoons. *Arch. Meteor. Geophys. Bioklimatol.*, **B29,** 245–252.
Parthasarathy, B., A. A. Munot, and D. R. Kothawale, 1995: Monthly and seasonal rainfall series for All-India homogenous regions and meteorological sub-divisions 1871–1994. IITM Research Rep. 65, Indian Institute of Tropical Meteorology, Pune, India, 113 pp.
Ramamurthy, K., 1969: Some aspects of ''break'' in the Indian south west monsoon during July and August. Forecasting Manual, Indian Meteorological Department Publication, FMU, Rep. 4, 18.3. [Available from Indian Meteorological Department, Mausam Bhavan, Lodi Road, New Delhi 110 003, India.]
Rasmusson, E. M., and T. H. Carpenter, 1983: The relationship between eastern equatorial Pacific sea surface temperature and rainfall over India and Sri Lanka. *Mon. Wea. Rev.,* **111,** 517–528.
Reynolds, R. W., and T. M. Smith, 1994: Improved global sea surface temperature analyses using optimum interpolation. *J. Climate,* **7,** 929–948.
Saji, N. H., B. N. Goswami, P. N. Vinayachandran, and T. Yamagata, 1999: A dipole mode in the tropical Indian Ocean. *Nature,* **401,** 360–363.
Shukla, J., 1975: Effects of Arabian Sea surface temperature anomaly on Indian summer monsoon: A numerical experiment with the GFDL model. *J. Atmos. Sci.,* **32,** 503–511.
——, and D. A. Paolino, 1983: The Southern Oscillation and long-range forecasting of the summer monsoon rainfall over India. *Mon. Wea. Rev.,* **111,** 1830–1837.
Sikka, D. R., 1999: Monsoon drought in India. Joint COLA/CARE Tech. Rep. 2, Center for Ocean–Land–Atmosphere Studies and Center for the Application of Research on the Environment, 243 pp.
——, and S. Gadgil, 1980: On the maximum cloud zone and the ITCZ over Indian longitudes during the southwest monsoon. *Mon. Wea. Rev.,* **108,** 1840–1853.
Smith, T. M., and R. W. Reynolds, 1998: A high-resolution global surface temperature climatology for the 1961–90 base period. *J. Climate,* **11,** 3320–3323.
Wang, B., 1988: Dynamics of tropical low-frequency waves: An analysis of the moist Kelvin wave. *J. Atmos. Sci.,* **45,** 2051–2065.
Washington, W. M., R. M. Chervin, and G. V. Rao, 1977: Effects of a variety of Indian Ocean surface temperature anomaly patterns on the summer monsoon circulation: Experiments with the NCAR general circulation model. *Pageoph,* **115,** 1335–1356.
Webster, P. J., J. P. Loschnigg, A. M. Moore, and R. R. Leben, 1999: Coupled ocean-atmosphere dynamics in the Indian Ocean during 1997–98. *Nature,* **401,** 356–359.
Weickmann, K. M., G. R. Lussky, and J. E. Kutzbach, 1985: Intraseasonal (30–60 day) fluctuations of outgoing longwave radiation and 250-mb streamfunction during northern winter. *Mon. Wea. Rev.,* **113,** 941–961.
Xie, P., and P. Arkin, 1997: Global precipitation: A 17-year monthly precipitation based on gauge observations, satellite estimates, and numerical model outputs. *Bull. Amer. Meteor. Soc.,* **78,** 2539–2558.
Yasunari, T., 1979: Cloudiness fluctuations associated with the Northern Hemisphere summer monsoon. *J. Meteor. Soc. Japan,* **57,** 227–242.
Zhang, C., 1993: Large-scale variability of deep convection in relation to sea surface temperature in the Tropics. *J. Climate,* **6,** 1898–1913.